Electrochemical Sensor for Rutin Detection with Graphene Oxide and Multi-Walled Carbon Nanotube Nanocomposite Modified Electrode

Lijun Yan, Xueliang Niu, Wencheng Wang, Xiaobao Li, Xiaohuan Sun, Caijuan Zheng, Jiewen Wang, Wei Sun[*]

Key Laboratory of Tropical Medicinal Plant Chemistry of Ministry of Education, College of Chemistry and Chemical Engineering, Hainan Normal University, Haikou 571158, P. R. China
[*]E-mail: swyy26@hotmail.com

A new modified electrode was prepared by dropping graphene oxide (GO) and multi-walled carbon nanotuble (MWCNT) nanocomposite on carbon ionic liquid electrode (CILE) surface, which was denoted as GO-MWCNT/CILE and further developed to establish electrochemical method for detecting rutin. Scanning election microscopy, cyclic voltammetry and electrochemical impedance spectroscopy were used to characterize the performance of GO-MWCNT/CILE. As compared with that of MWCNT/CILE, GO/CILE and the bare CILE, the redox peak currents of rutin on GO-MWCNT/CILE increased, which was ascribed to the large surface area and good electron transfer performance of GO-MWCNT nanocomposite on the electrode surface. At GO-MWCNT/CILE the oxidation peak currents of rutin increased proportional to the concentration within the range of 0.08~80.0 μmol L^{-1} accompanied by the detection limit of 0.02 μmol L^{-1} (3σ). Furthermore, the analytical application of the present approach for rutin tablets was evaluated with good sensitivity and acceptable recoveries.

1. INTRODUCTION

As an important member of bioactive flavonoids, rutin (3', 4', 5, 7-tetrahydroxyflavone 3β-D-rutinoside) is widely presented naturally in many plants. Owing to its promising physiological activities including anti-tumor, anti-cancer, anti-inflammatory and anti-bacteria etc, rutin has been used in clinically, acting as a therapeutical medicine for anti-cogalant and lowing blood pressure etc.[1]. Therefore it is very important to find a sensitive analytical approach for rutin determination in

pharmaceutical drugs or plants. Up to now, many analytical techniques have been explored for this purpose, such as UV-Vis spectrophotometry [2], high-performance liquid chromatography [3], flow injection analysis [4], capillary zone electrophoresis [5], chemiluminescence [6], electrochemiluminescence [7] and electrochemical methods [8,9]. However some of traditional methods have the disadvantages such as complex operation, high cost, large amounts of toxic organic solvents used, separation process, time-consuming and so forth. With the merits of high sensitivity, good stability, simple and quick operation, low cost equipment and wide dynamic range, electroanalytical techniques have been used in flavonoids investigation. Because rutin is an electroactive flavonoid glycoside compound that can be easily subject to either redox reaction on different kinds of working electrodes, therefore it can be detected by various electrochemical methods. Also chemically modified electrodes with various modifiers have been explored for the determination of rutin with enhanced sensitivity. For example Wei et al. fabricated a CeO_2 nanoparticle modified electrode to recognize and detect rutin [10]. Zoulis et al. detected rutin and other flavonoids by adsorptive stripping voltammertry with preconcentration using carbon paste electrode (CPE) as working electrode [11]. Sun et al. constructed a carbon ionic liquid electrode (CILE) and further applied to investigate the electrochemical behaviors of rutin [12]. Electrochemical behaviors of rutin was also investigated on a nitrogen-doped graphene modified CILE [13].

With the structural characteristic of a two-dimensional monolayer of sp^2 carbon atoms, graphene (GR) has been a promising sensing material owing to its specific properties including large surface area, unique electrochemical properties, excellent electron transfer rate, high mobility of charge carriers and good mechanical strength [14,15]. The synthesis and applications of GR in various fields such as supercapacitor, energy storage, chemical sensor and biosensor had been reviewed in recent years [16-18]. However GR tends to aggregate back to graphite because of the strong π-π interaction and *van der waals*, which resulted in its limitation in applications. As the most important precursor of GR, graphene oxide (GO) has also attracted infinite interests due to its good solubility with many functional groups. GO is a non-stoichiometric two-dimensional carbon nanomaterial that resulted from the acid exfoliation of natural graphite, which exhibits the properties such as facile surface modification, good water dispersibility and high mechanical strength. Dreyer et al. reviewed the chemistry of GO, which could act as a substrate for the further chemical transformations [19]. Due to the presence of epoxide and hydroxyl functional groups on the based plane and carboxyl groups on the edge sites, GO can be used for the further modification by ionic or nonionic interaction with the formation of novel hybrid materials [20,21]. Balapanuru et al. applied a GO-organic dye ionic complex for the DNA sensing [22]. Wang et al. investigated the biocompatibility of GO by studying the effects of GO on human fibroblast cells and mice [23]. Lu et al. demonstrated the fluorescence quenching properties of GO in DNA biosensing [24]. But the presences of oxygenal groups on GO nanosheets can decrease the electrical conductivity and limit the application in the field of electrochemistry. As another carbon nanomaterial that has been widely investigated, carbon nanotube (CNT) exhibits excellent properties such as high electrical conductivity, large surface area and excellent electrocatalytic activity, which has been utilized in the domain of electrochemistry and electrochemical sensors [25, 26]. Wang et al. reviewed the progresses of CNT based electrochemical biosensor [27]. Vashist et al. summarized the advances of CNT based electrochemical sensors for the bioanalytical

applications [28]. However CNT tends to agglomerate in organic dispersion, so great efforts have been developed to disperse CNT by using micelles, ionic liquid and so on. Recently GO has been proved to be a better dispersant for CNT, which can result in a stable dispersion hybrid nanocomposite [29]. The strong π-π stacking interaction between GO and CNT can result in a stable hybrid with many specific characteristics including higher conductivity, larger specific area and excellent catalytic properties. Mani et al. reviewed the recent progress in the preparation of GO-CNT hybrid nanomaterials and their applications in different fields such as supercapacitors, dye sensitized solar cells, sensors and batteries [30]. The combination of 2D GO and 1D CNT can generate a versatile 3D GO-CNT hybrid network with synergistic effects. Tian et al. prepared a stable GO and single-walled CNT (SWCNT) hybrid by ultrasonication [31]. Kim et al. applied a GO-SWCNT composite modified glassy carbon electrode (GCE) as the anode for polymer solar cells [32]. Li et al. fabricated a GO-CNT modified GCE for the sensitive electrochemical determination of L-lyrosine [33]. Zhu et al. applied a multi-walled CNT (MWCNT)-aminate reduced GO hybrid modified GCE for the voltammetric detection of rutin [34]. Zhang et al. realized the direct electrochemistry of horseradish peroxidase on GO/MWCNT nanocomposite modified electrode [35]. Therefore GO-CNT nanocomposites have the wide potential applications in chemically modified electrodes.

Herein GO-MWCNT nanocomposite was prepared by ultrasonication approach and further modified on the surface of CILE. With the advantages of good anti-fouling ability, wide potential range and certain electrocatalytic activity, CILE has been used in the field of electrochemical sensor [36,37]. Because of the good solubility and high viscosity of IL used as the modifier in CILE fabrication, a IL film can be formed on the surface of carbon powder. Then the cation-π interaction and/or non-covalent π-π electronic stacking, hydrophobic, or electrostatic interaction between the IL molecules and GO-MWCNT nanocomposite were present, which led to a stable membrane on the electrode surface. GO-MWCNT/CILE was applied for the investigation on the electrochemical behaviors of rutin. Due to the synergistic effects of GO, MWCNT and their interaction with IL, electrochemical responses of rutin were greatly enlarged. Therefore a new sensitive voltammetric approach for analysis of rutin was further conceived and applied to the drug samples determination with high sensitivity, selectivity and good recovery.

2. EXPERIMENTAL PART

2.1. Chemicals

Ionic liquid 1-hexylpyridinium hexafluorophosphate (HPPF$_6$, Lanzhou Greenchem. ILS. LICP. CAS., China), graphite powder (average particle size 30 μm, Shanghai Colloid Chem. Ltd. Co., China), graphene oxide (GO, Taiyuan Tanmei Ltd. Co., China) MWCNT (purity > 95%, main range of diameter < 10 nm, length of 5~15 μm, Shenzhen Nanoport. Co., China) and rutin (Sinopharm. Chem. Reagent Ltd. Co., China) were utilized directly. The supporting electrolyte was 0.1 mol L^{-1} phosphate buffer solution (PBS) and the pH values were adjusted with 0.1 mol L^{-1} HCl or 0.1 mol L^{-1} NaOH.

Other chemicals used in this study were all of analytical reagent grade and used as received. Doubly distilled water was used throughout the experiments.

2.2. Apparatus

A CHI 750B electrochemical workstation (Shanghai CH Instrument, China) was used to carry out all the electrochemical experiments. A conventional three-electrode system was used with a GO-MWCNT/CILE as the working electrode, a platinum wire as the auxiliary electrode and a saturated calomel electrode (SCE) as the reference electrode. Scanning electron microscopy (SEM) was performed on JSM-7600F scanning electron microscope (JEOL, Japan).

2.3. Fabrication of GO-MWCNT/CILE

CILE was prepared according to a previous work we had reported [38]. In brief, 0.8 g of $HPPF_6$ and 1.6 g of graphite powder were mixed in a mortar and ground carefully to get a homogeneous paste, which was packed into a glass tube (Φ=4.2 mm) and the electrical contact was established through a copper wire to the end of the paste. Then the surface of CILE was polished on a weighing paper just before use.

A 1.0 mL solution that contained 0.7 mg of MWCNT and 0.3 mg of GO was mixed homogeneously and ultrasonicated for 1 h to get a suspension solution. And then 5 μL of solution was evenly dropped onto the surface of CILE and left it vapor to dry at ambient temperature. The modified electrode was denoted as GO-MWCNT/CILE, which was kept at 4 ^{o}C refrigerator when it was not in use. In order to compare the performance of different modified electrodes, CILE, GO/CILE and MWCNT/CILE were also fabricated with the similar procedures.

2.4. Electrochemical procedure

Electrochemical measurements, including cyclic voltammetry (CV), differential pulse voltammetry (DPV) and electrochemical impedance spectroscopy (EIS), were carried out at room temperature (20 ^{o}C ± 2 ^{o}C) with a CHI 750B electrochemical workstation. All the cyclic voltammetric experiments were performed in PBS containing certain amount of rutin at the scan rate of 100 mV s^{-1}. Differential pulse voltammograms were recorded in the potential range from 0.2 V to 0.8 V with the instrumental parameters set as: pulse amplitude 0.005 V, pulse width 0.05 s and pulse period 0.2 s.

3. RESULTS AND DISCUSSION

3.1. SEM images

SEM images of nanomaterials on the surface of CILE was recorded and listed in Figure 1. As shown in Figure 1A, the GO film on CILE demonstrated a typical crumpled and corrugated appearance

with a wrinkled silk structure, indicating the existence of GO nanosheet on CILE surface. While on MWNCT/CILE (Figure 1B) it can be observed that MWCNT was entangled with each other to form a network and porous framework. As for that of GO-MWCNT/CILE (Figure 1C), different appearance appeared with MWCNT mixed with GO evenly to get a hybrid. MWCNT was present on the surface of GO and the porous structure of MWCNT was inserted by GO nanosheet. GO nanosheet is an amphiphile with hydrophilic edges to keep its solubility and hydrophobic basal plane to bond with CNT by the π-π interaction [39]. The SEM results showed that GO and MWCNT could form a homogeneously hybrid.
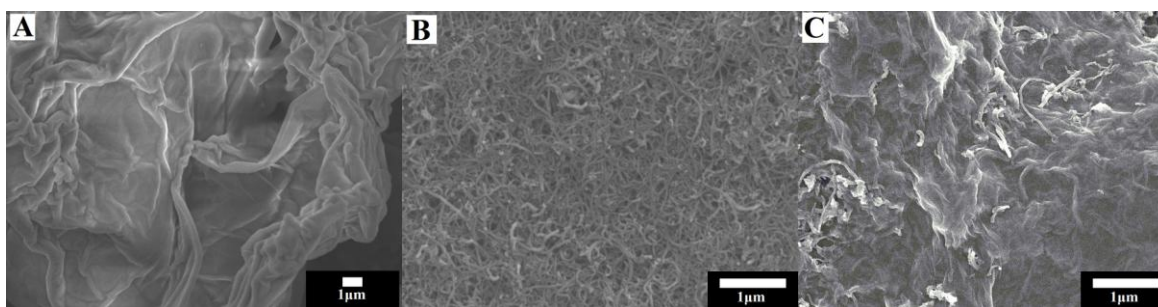

Figure 1. SEM images of GO/CILE (A), MWCNT/CILE (B) and GO-MWCNT/CILE (C).

3.2. Electrochemical characteristics of the modified electrodes

Electrochemical characteristics of the modified electrodes were explored by EIS and CV with the results shown in Figure 2. As a powerful technique for the analysis of the impedance changes of the electrode, EIS is commonly applied to explore the interfacial information. The typical Nyquist polt of EIS is composed of a semicircle portion and a linear portion, which is corresponding to the electron transfer limited process and the diffusion limited process. The value of the electron transfer resistance (Ret) depends on the dielectric and insulation characteristics at the electrode/electrolyte interface, which can be estimated from the diameter of the semicircle of the Nyquist plots. Z′ and Z″ are the real variable and the negative value of the imaginary variable of the impedance. Figure 2A showed the EIS results of different modified electrodes in a 10.0 mmol L^{-1} $[Fe(CN)_6]^{3-/4-}$ and 0.1 mol L^{-1} KCl mixture solution with the frequency swept from 10^4 to 0.1 Hz. On CILE the Ret value was got as 110.46 Ω (curve b) and that of GO/CILE was increased to 196.50 Ω (curve a), indicating that the presence of GO nanosheet on the CILE surface increased the interfacial resistance and hindered the electron transfer. Because of the presence of oxygenal groups on the GO nanosheet, the electrical conductivity of GO is poor and the Ret value of the GO modified electrode increased correspondingly. While on MWCNT/CILE the Ret value decreased to 43.14 Ω (curve c), which could be attributed to the presence of high conductive MWCNT on the CILE surface that facilitated the electron transfer. On GO-MWCNT/CILE the Ret value decreased to the smallest value with a straight line appeared (curve d), indicating that the synergistic effects of GO and MWCNT increased the interfacial conductivity. The combination of 1D CNT with 2D GO nanosheet can result in a 3D GO-CNT hybrid composite, which exhibits the merits of GO and CNT simultaneously [30]. The presence of CNT in the composite can

expand the layer distance of GO nanosheet, act as wires to bridge the defect of GO for electron transfer, fill in the vacancies and form a 3D conductive network. The network structure can be served as the fast electronic and ionic conducting channels for the analytes [40]. Therefore a high conductive pathway and interface could be formed on the electrode for electron transfer with the smallest Ret value.

Cyclic voltammograms of different electrodes were further recorded in a 1.0 mmol L^{-1} [Fe(CN)$_6$]$^{3-/4-}$ solution with the results shown in Figure 2B. On CILE a pair of well-defined redox peaks appeared (curve b), which indicated that CILE was an excellent working electrode due to the presence of high ionic conductive IL on the electrode [36, 37]. After the casting of GO on CILE, the redox peak currents decreased (curve a), which indicated that the less conductive GO nanosheet on the electrode surface decreased the interfacial conductivity. On MWCNT/CILE (curve c) the redox peak currents increased greatly, indicating the presence of high conductive MWCNT was beneficial for the electron transfer. On GO-MWCNT/CILE the biggest redox peak currents appeared (curve d), which could be attributed to the presence of GO-MWCNT hybrid nanocomposite that exhibited excellent electrochemical properties for the electron transfer. The interaction of GO and MWCNT can form a stable hybrid due to the strong π-π interaction. While on the surface of CILE a layer of IL is present due to its high viscosity and good solubility. The IL molecules can also interact with GO-MWCNT nanocomposite through π-π, π-cationic, hydrophobic interaction, which result in a stable carbon nanomaterial-IL film surface [41,42]. The co-contribution of GO-MWCNT and IL on the electrode surface can act as an efficient promoter to enhance the electron transfer.
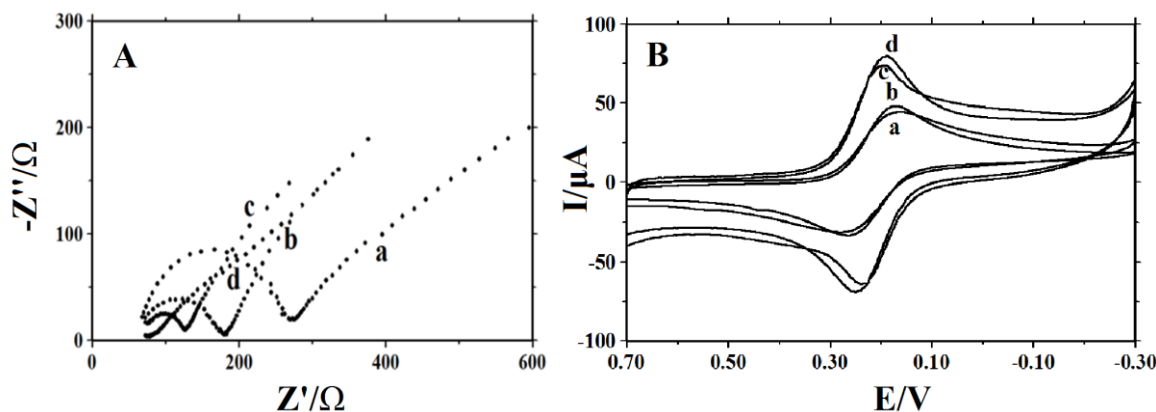

Figure 2. (A) EIS of (a) GO/CILE, (b) CILE, (c) MWCNT/CILE and (d) GO-MWCNT/CILE in a 10.0 mM [Fe(CN)$_6$]$^{3-/4-}$ and 0.1 M KCl solution with the frequency ranged from 10^4 to 0.1 Hz; (B) Cyclic voltammograms of (a) GO/CILE, (b) CILE, (c)MWCNT/CILE and (d) GO-MWCNT/CILE in a 1.0 mmol L^{-1} [Fe(CN)$_6$]$^{3-/4-}$ and 0.5 mol L^{-1} KCl solution with scan rate as 100 mV s^{-1}.

The mass ratio of GO and MWCNT for the preparation of GO-MWCNT hybrid were investigated by cyclic voltammetry in the [Fe(CN)$_6$]$^{3-/4-}$ solution. The ratio of GO:MWCNT was selected as 1:9, 2:8, 3:7, 4:6, 5:5, 6:4, 7:3, 8:2 and 9:1, and the best ratio of 3:7 was chosen with the biggest voltammetric responses appeared. When the amount of CNT is less, the whole conductivity of

hybrid is poor due to the less conductivity of GO nanosheet. When the amount of CNT is big, the hybrid is not stable due to the hydrophobicity of CNT. Therefore the optimal mass ratio of GO and MWCNT was selected as 3:7 for the preparation of the hybrid.

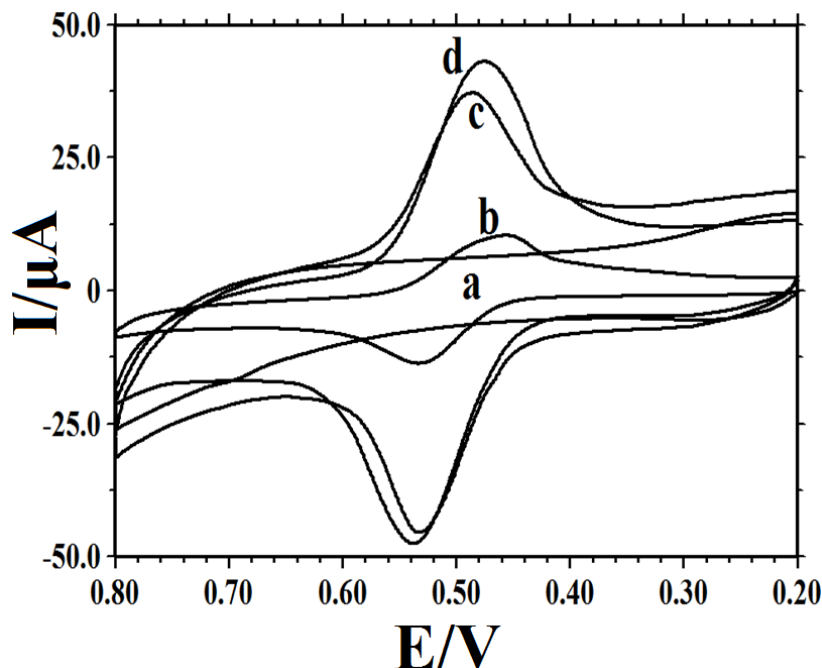*3.3. Electrochemical behaviors of rutin on the modified electrodes*

Figure 3. Cyclic voltammograms of (a) GO-MWCNT/CILE in the buffer solution, (b) CILE, (c) MWCNT/CILE and (d) GO-MWCNT/CILE in pH 2.5 PBS containing 50.0 μmol L^{-1} rutin with scan rate as 100 mV s^{-1}.

Electrochemical responses of rutin on different modified electrodes were studied by CV with the results shown in Figure 3. It was obviously that no responses appeared on GO-MWCNT/CILE in pH 2.5 PBS (curve a), indicating that the modifier was inactive and GO-MWCNT/CILE could remain stable in the supporting electrolyte solution. While for 50.0 μmol L^{-1} rutin solution a pair of well-defined redox peaks appeared on each electrode, which can be ascribed to the redox behaviors of rutin at the working electrode. Rutin has been elucidated with a two-electron and two-proton electrochemical process, and the electrode reaction can be influenced by the modifiers on the modified electrode [9]. On CILE (curve b) the smallest electrochemical signals could be observed and the electrochemical responses increased greatly on MWCNT/CILE (curve c). The result can be attributed to the presence of MWCNT on the electrode surface that could act as the effective mediator to promote the electrochemical reaction of rutin. While the biggest redox peaks appeared on GO-MWCNT/CILE (curve d) with the ΔE_p value as 38 mV, which indicated that GO-MWCNT hybrid on the electrode surface exhibited the best electrocatalytic ability with fast electron transfer rate. In GO-MWCNT hybrid MWCNT can serve as the spacer to enlarge the distance between GO nanosheet and act as a conductive wire to compensate the electric conductivity of GO. While GO nanosheet can provide large surface area to prevent the agglomerate of MWCNT. Also the network GO-MWCNT hybrid can

provide a higher porosity structure and efficient diffusion pathways for the electrolyte and the analyte. Therefore GO-MWCNT/CILE exhibited an improved performance due to the synergistic effects of GO and MWCNT in the composite.

3.4. Influence of buffer pH

The influence of acidity on the cyclic voltammetric responses of 10.0 µmol L^{-1} rutin was investigated by changing the buffer pH from 1.5 to 5.0 with cyclic voltammograms shown in Figure 4. In the meantime the relationships of the formal peak potential ($E^{0'}$) and the oxidation peak current (I_{pa}) with buffer pH were plotted and shown in Figure 4B and 4C. The redox peak potential moved negatively while the buffer acidity decreased, indicating that protons were involved in the electrode reaction. The linear regression equation of $E^{0'}$ depend on pH was got as $E^{0'}$ (V) = -0.052 pH + 0.66 (γ = 0.997) with a slope value of -52 mV pH^{-1}, which was approximately equal to the theoretical value of - 59 mV pH^{-1} [42]. By the equation [43], -59.0 x/n = -52.0, where x is the proton involved in the electrode reaction and n is the number of electron transferred. Therefore the ratio of x/n is close to 1, which indicates that the same amount of electron and proton involved in the electrode reaction. In the solution pH range of 1.5~5.0, the I_{pa} value increased from 1.5 to 2.5 and then decreased with the maximum value got at pH 2.5 (Figure 4C). Therefore pH 2.5 was selected as the optimal pH for the following experiments. At this acidic solution more protons can be supplied for the electrochemical reaction of rutin with fast reaction rate.
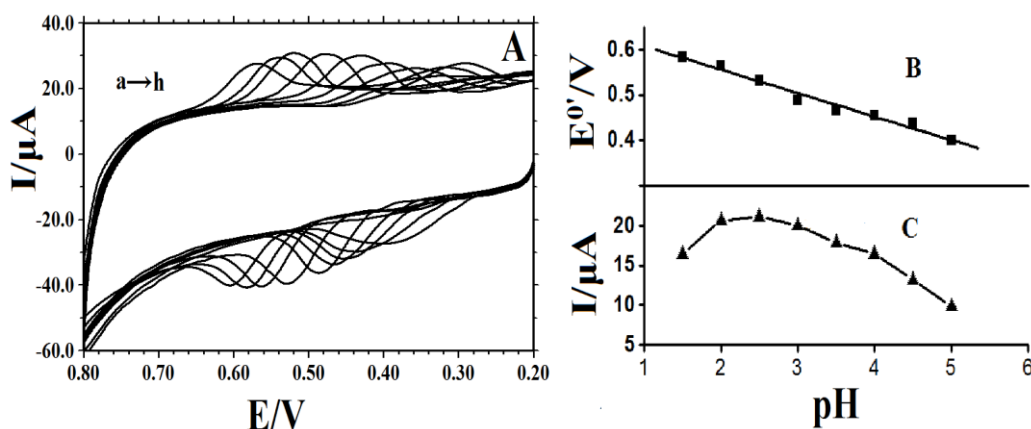

Figure 4. (A) Cyclic voltammograms of 10.0 µmol L^{-1} rutin on GO-MWCNT/CILE with different pH PBS (from a to i are 1.5, 2.0, 2.5, 3.0, 3.5, 4.0, 4.5, 5.0, respectively), scan rate: 100 mV s^{-1}; (B) The relationship between the formal peak potential ($E^{0'}$) and pH; (C) The relationship between the oxidation peak current (I_{pa}) and pH.

3.5. Effect of scan rate

In a 50.0 µmol L^{-1} rutin solution, the influence of scan rate on the electrochemical response of rutin at GO-MWCNT/CILE was investigated. As shown in Figure 5, when scan rate increased from

30.0 to 500.0 mV s^{-1}, the redox peak currents increased correspondingly with the movement of the redox peak potentials. Good linear relationship between the redox peak currents (I_p) and scan rate (v) were plotted (Figure 5B) with two regression equations as I_{pc} (μA) = 180.44 v + 0.556 (γ = 0.999) and I_{pa} (μA) = -219.46 v - 2.794 (γ = -0.999), indicating an adsorption-controlled electrode process. The adsorption of rutin at the surface of GO-MWCNT/CILE can be attributed to the π-π interaction of the benzene ring of rutin with the benzene ring of the GO-MWCNT hybrid. The redox peak potentials dependence on ln$v$ obeyed the equations E_{pc} (V) = -0.0221 ln$v$ + 0.430 (γ = -0.984) and E_{pa} (V) = 0.0236 ln$v$ + 0.568 (γ = 0.975), respectively. Based on the following equations [44],

$$Epc = E^{0'} - \frac{RT}{\alpha nF} \ln v \qquad (1)$$

$$Epa = E^{0'} + \frac{RT}{(1-\alpha)nF} \ln v \qquad (2)$$

$$\log k_s = \alpha \log(1-\alpha) + (1-\alpha)\log \alpha - \log \frac{RT}{nFv} - \frac{(1-\alpha)\alpha nF \Delta Ep}{2.3RT} \qquad (3)$$

The possible redox reaction parameters could be calculated with the slopes of the lines expressed as RT/(1-α)nF for E_{pa} and RT/αnF for E_{pc}, where α and n were the symbols of charge transfer coefficient and number of electron transferred. Therefore, α, n and k_s (electrode reaction standard rate constant) were calculated as 0.48, 2.2 and 1.85 s^{-1}, respectively. The n value of 2.2 is close to the reported theoretical value (2) for the electrochemical reaction of rutin [9]. Therefore the protons taken part in the electrode reaction were also deduced as 2.
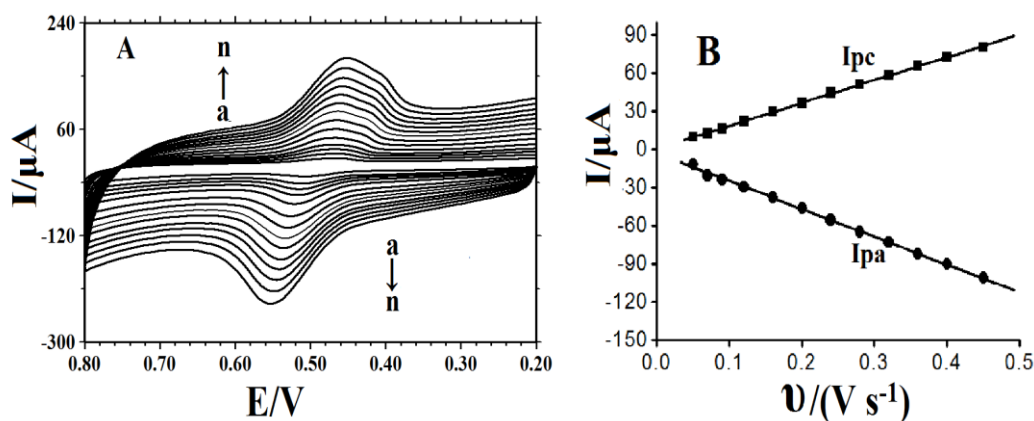

Figure 5. (A) Cyclic voltammograms of 50.0 μmol L^{-1} rutin with different scan rate (v) on GO-MWCNT/CILE in pH 2.5 PBS (from a to n are 30, 50, 70, 90, 120, 160, 200, 240, 280, 320, 360, 400, 450, 500 mV s^{-1}, respectively); (B) Linear relationship of the redox peak current (I_p) versus v.

3.6. Working curve

Under the optimized experimental parameters, the relationship of oxidation peak currents with rutin concentration was investigated by DPV for its better sensitivity than CV with the typical voltammograms shown in Figure 6. It can be seen that the linearity between I_{pa} value and rutin

concentrations covered the range of 0.08~10.0 μmol L^{-1} and 10.0~80.0 μmol L^{-1}. The equations could be expressed as I_{pa} (μA) = 1.448 + 3.169 C (μmol L^{-1}) (γ = 0.988) and I_{pa} (μA) = 32.06 + 0.225 C (μmol L^{-1}) (γ = 0.991), respectively. The detection limit was 0.02 μmol L^{-1} (3σ), which was lower than some previous reported values [9-12]. The lower detection limit was attributed to the better performance of GO-MWCNT hybrid with synergistic effects, such as the large surface area and the network of GO-MWCNT hybrid with the adsorption of rutin as well as certain electrcatalytic effect. The relative standard deviation (RSD) of 11 successive determinations of 10.0 μmol L^{-1} rutin had the result of 3.18 %, indicating that GO-MWCNT/CILE exhibited good reproducibility for voltammetric detection. The repeatability was studied in terms of detecting 10.0 μmol L^{-1} rutin solution using five modified electrodes that were fabricated independently. A satisfactory RSD value of 3.5 % was got, indicating the good repeatability.
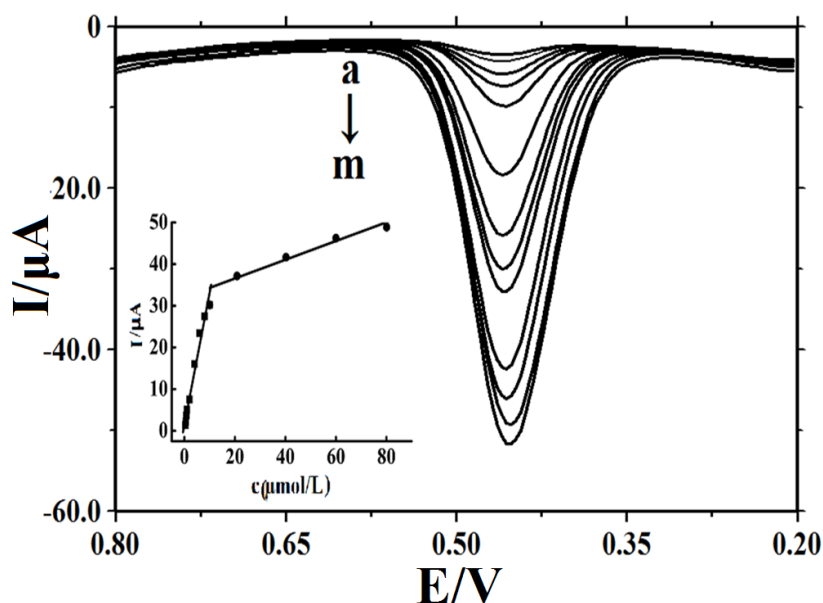

Figure 6. Differential pulse voltammograms of various concentrations rutin on GO-MWCNT/CILE (from a to m are: 0.080, 0.20, 0.40, 0.60, 0.80, 2.0, 4.0, 6.0, 8.0, 20.0, 40.0, 60.0, 80.0 μmol L^{-1}); Inset is the relationship of the I_{pa} with rutin concentration.

3.7. Sample determination

With the purpose of ascertain the potential application, the proposed method based on GO-MWCNT/CILE was utilized to analyze rutin content in tablet samples (20 mg tablet^{-1}), which were supplied by Shanxi Yunpeng Pharmaceutical Co. Ltd. (B080302) and Shanghai Zhaohui Pharmaceutical Co. Ltd. (090904). The process for preparing rutin samples solution were as following: two tablets of rutin were carefully ground in the agar, transferred to a 10 mL calibrated tube and diluted to the scale with ethanol. A 100 μL solution was further diluted with pH 2.5 PBS in a 10 mL calibrated tube and then detected by the experimental procedure. Meanwhile the recovery was also tested with the standard addition method to assess the accuracy of the present method. The results were

all listed Table 1, which showed that the recovery was got in the range of 99.66~100.33%. Therefore the modified electrode could be efficiently applied for rutin analysis in commercial pharmaceutical samples.

Table 1. Determination results of rutin content in tablet samples (n=3)

Sample	Specified (μmol L^{-1})	Detected (μmol L^{-1})	Added (μmol L^{-1})	Total (μmol L^{-1})	RSD (%)	Recovery (%)
B080302	60.2	59.1	30.0	89.0	1.29	99.66±0.22
090904	60.2	60.5	30.0	91.5	2.47	100.33±0.38

4. CONCLUSION

In this study GO-MWCNT hybrid was prepared by a simple ultrasonication method in aqueous solution, which was further casted on the surface of CILE. The modified electrode showed better electrochemical performances due to the presence of GO-MWCNT hybrid and its interaction with IL on the electrode. The synergistic effects of 2D GO and 1D MWCNT resulted in 3D network nanocomposite that was benefit for the efficient transport of electrons and facilitated the electrochemical reaction of rutin. Under the optimal experimental parameters, the linearity between I_{pa} value and rutin concentrations covered the range from 0.080 to 80.0 μmol L^{-1} with the detection limit as 0.02 μmol L^{-1} (3σ). The GO-MWCNT/CILE was further utilized to analyze rutin tablet samples with high sensitivity, excellent reproducibility and good stability, which provided a novel sensing platform for rutin detection.

References

1. R.M. Gené, C. Cartañá, T. Adzet, E. Marín, T. Parella and S. Cañigueral, *Planta Med*. 62 (1996) 232.
2. H. Xu, Y. Li, H.W. Tang, C.M. Liu and Q.S. Wu, *Anal. Lett*. 43 (2010) 893.
3. I. Kazuo, F. Takashi and K. Yasuji, *J. Chromatogr. B. Biomed. Appl*. 759 (2001) 161.
4. C.X. He, X.Y. Zhao, H.Z. Zha and G.W. Zhao, *Anal. Lett*. 32 (1999) 2751.

5. Q.J. Wang, F. Ding, H. Li, P.G. He and Y.Z. Fang, *J. Pharmaceut. Biomed. Anal.* 30 (2003) 1507.
6. Z.H. Song and S. Hou, *Talanta* 57 (2002) 59.
7. Y.D. Liang and J.J. Song, *J. Electroanal. Chem.* 624 (2008) 27.
8. J. Lou, L.J. Yan, W.C. Wang, C.X. Ruan, A.H. Hu and W. Sun, *J. Chin. Chem. Soc.* 62 (2015) 640.
9. Y. Wei, G.F. Wang, M.G. Li, C. Wang and B. Fang, *Microchim. Acta* 158 (2007) 269.
10. J.W. Kang, X.Q. Lu, H.J. Zeng, H.D. Liu and B.Q. Lu, *Anal. Lett.* 35 (2002) 677.
11. N.E. Zoulis and C.E. Efstathiou, *Anal. Chim. Acta* 320 (1996) 255.
12. W. Sun, M.X. Yang, Y.Z. Li, Q. Jiang, S.F. Liu and K. Jiao, *J. Pharmaceut. Biomed. Anal.* 48 (2008) 1326.
13. W. Sun, L.F. Dong, Y.X. Lu, Y. Deng, J.H. Yu, X.H. Sun and Q.Q. Zhu, *Sensor. Actuator. B.* 199 (2014) 36.
14. C. Srinivasan, *Curr. Sci. India* 92 (2007) 1338.
15. A.K. Geim and K.S. Novoselov, *Nat. Mater.* 6 (2007) 183.
16. M. Pumera, *Chem. Soc. Rev.* 39 (2010) 4146.
17. J.Q. Liu, Z. Liu, C.J. Barrow and W.R. Yang, *Anal. Chim. Acta.* 859 (2015) 1.
18. A.T. Lawal, *Talanta* 131 (2015) 424.
19. D.R. Dreyer, S.J. Park, C.W. Bielawski and R.S. Ruoff, *Chem. Soc. Rev.* 39 (2010) 228.
20. Y.Y. Liang, D.Q. Wu, X.L. Feng and K. Mllen, *Adv. Mater.* 21 (2009) 1679.
21. X.L. Li, G.Y. Zhang, X.D. Bai, X.M. Sun, X.R. Wang, E. Wang and H.G. Dai, *Nat. Nanotechnol.* 3 (2008) 538.
22. J. Balapanuru, J.W. Yang, S. Xiao, Q.L. Bao, M. Jahan, L. Polavarapu, J. Wei, Q.H. Xu and K.P. Loh, *Angew. Chem. Int. Edit.* 49 (2010) 6549.
23. K. Wang, J. Ruan, H. Song, J.L. Zhang, Y. Wo, S.W. Guo and D.X. Cui, *Nanoscale Res. Lett.* 6 (2011) 8.
24. C.H. Lu, H.H. Yang, C.L. Zhu, X. Chen and G.N. Chen, *Angew. Chem. Int. Edit.* 48 (2009) 4785.
25. T. L. Abdulazeez, *Mater. Res. Bull.,* 73 (2016) 308.
26. P. Yanez-Sedeno, J.M. Pingarron, J. Riu and F.X. Rius, *Trac-Trend. Anal. Chem.* 29 (2010) 939.
27. J. Wang, Electroanal. 17 (2005) 7.
28. S.K. Vashist, D. Zheng, K. Al-Rubeaan, J.H.T. Luong and F.S. Sheu, *Biotechnol. Adv.* 29 (2011) 169.
29. V. Mani, B. Devadas and S.M. Chen, *Biosens. Bioelectron.* 41 (2013) 309.
30. V. Mani, S.M. Chen and B.S. Lou, *Int. J. Electrochem. Sci.* 8 (2013) 11641.
31. L. Tian, M.J. Meziani, F. Lu, C.Y. Kong, L. Cao, T.J. Thorne and Y.P. Sun, *ACS Appl. Mater. Inter.* 2 (2010) 3217.
32. J. Kim, V.C. Tung and J. Huang, *Adv. Energy Mater.* 1 (2011) 1052.
33. J. Li, D. Kuang, Y. Feng, F. Zhang, Z. Xu, M. Liu and D. Wang, *Microchim. Acta* 180 (2013) 49.
34. X.F. Zhu, J.K. Xu, X.M. Duan, L.M. Lu, H.K. Xing, Y.S. Gao, H. Sun, L.Q. Dong and T.T. Yang, *Int. J. Electrochem. Sci.* 10 (2015) 9192.
35. Q. Zhang, S. Yang, J. Zhang, L. Zhang, P. Kang, J. Li, J. Xu, H. Zhou and X.M. Song, *Nanotechnology* 22 (2011) 494010.
36. W. Sun, R.F. Gao and K. Jiao, *Chin. J. Anal. Chem.* 35 (2007) 1813.
37. J.A.M. Shiddiky and A.A.J. Torriero, *Biosens. Bioelectron.* 26 (2011) 1775.
38. X.F. Wang, Z.You, Y. Cheng, H.L. Sha, G.J. Li, H.H. Zhu and W. Sun, *J. Mol. Liq.,* 204 (2015) 112.
39. Q.B. Zheng, B. Zhang, X.Y. Lin, X. Shen, N. Yousefi, Z.D. Huang, Z.G. Li and J.K. Kim, *J. Mater. Chem.* 22 (2012) 25072.
40. D.S. Yu and L.M. Dai, *Chem. Lett.* 1 (2010) 467.
41. S.R. Ng, C.X. Guo and C.M. Li, *Electroanalysis* 23 (2011) 442.
42. P. Rahimi, H. Rafiee-Pour, H. Ghourchian, P. Norouzi and M. Ganjali, *Biosens. Bioelectron.* 25 (2009) 1301.

43. R.S. Nicholson, *Anal. Chem*. 37 (1965) 1351.
44. J. Wang, *Analytical electrochemistry*, third ed. John Wiley and Sons, Hoboken, New Jersey (2006).